

Reproducibility of 3.0T High-Resolution Magnetic Resonance Imaging for the Identification and Quantification of Middle Cerebral Arterial Atherosclerotic Plaques

Deng-Ling Zhao, MD, PhD, Cheng Li, MD, Xiao-Hui Chen, MD, Shenghong Ju, MD, PhD, Gang Deng, MD, PhD, Bo Xie, PhD, and Gao-Jun Teng, MD, PhD

Objective: To assess the reproducibility of 3.0T high-resolution magnetic resonance imaging for the identification and quantification of atherosclerotic plaques in the middle cerebral artery. *Methods:* Sixty-nine consecutive patients with ischemic stroke or asymptomatic stenosis (>30%) of the middle cerebral artery underwent 3.0T high-resolution magnetic resonance imaging examinations. Two independent investigators reviewed all images with 1 investigator re-evaluating all images 4 weeks later. Wall characteristics of the middle cerebral artery, including plaque surface morphology, plaque location, plaque components, and burden were identified and measured. *Results:* Intraobserver and interobserver agreement were all substantial in identifying plaque surface irregularity ($k = 0.741, 0.555-0.897$; $k = 0.685, 0.490-0.843$; respectively) and intraplaque hemorrhage ($k = 0.654, 0.446-0.838$; $k = 0.605, 0.369-0.792$; respectively). Intraobserver agreement was substantial ($k = 0.654$) and interobserver agreement was moderate ($k = 0.553$) for the identification of plaque fibrous caps. The total intraobserver and interobserver reproducibility was almost excellent for the identification of plaque position. With regards to vessel area measurement at the site of maximal lumen narrowing, intraobserver and interobserver reproducibility was excellent (intraclass correlation coefficient was 0.886 and 0.885, respectively) and moderate for lumen area at the site of maximal lumen narrowing (intraclass correlation coefficient was 0.695 and 0.558, respectively). In addition, intraobserver and interobserver reproducibility was excellent for vessel area and lumen area measurements at the reference sites. *Conclusions:* The reproducibility of 3.0T high-resolution magnetic resonance imaging for the identification and quantification of artery wall characteristics was overall acceptable. However, the reliability for lumen area measurement at the maximum narrowing site and identification of the fibrous cap needs to be improved.

Key Words: Middle cerebral artery—atherosclerosis—magnetic resonance imaging—high resolution—reproducibility
© 2019 Published by Elsevier Inc.

Introduction

Intracranial atherosclerotic disease is the most frequent cause of ischemic stroke in patients of Asian descent.¹ The

middle cerebral artery (MCA) is the area that is most predominantly affected with an overall annual stroke risk being 12.5% in patients with symptomatic MCA stenosis.²

From the Department of Radiology, Zhongda Hospital, Medical School, Southeast University, Nanjing, Jiangsu Province, China. Received December 17, 2018; revision received March 24, 2019; accepted April 14, 2019.

Financial Disclosure: This work was funded by the Natural Science Foundation of Jiangsu Province of China (BK20170704), the program of Jiangsu Provincial Commission of health and family planning of China (H2017008) and the Clinical Innovation Center of Medical Imaging and Interventional Radiology of Jiangsu Province of China (YXZX2016005).

Address correspondence to: Gao-Jun Teng, MD, PhD, Department of Radiology, Zhongda Hospital, Medical School, Southeast University, 87 Dingjiaqiao Road, Gulou District, Nanjing, Jiangsu Province, China. E-mail: gjteng@vip.sina.com.

1052-3057/\$ - see front matter

© 2019 Published by Elsevier Inc.

<https://doi.org/10.1016/j.jstrokecerebrovasdis.2019.04.020>

Imaging modalities such as digital subtraction angiography, computed tomography angiography, and magnetic resonance angiography (MRA) are the most commonly used diagnostic tools to evaluate atherosclerotic stenosis of intracranial arteries. However these vascular imaging modalities only display luminal narrowing and are unable to provide information on the underlying pathology within the vessel wall.³

Lately, high-resolution magnetic resonance imaging (HR MRI) has emerged as a novel diagnostic technique that provides *in vivo* information on atheroma and artery wall characteristics. Several small cohort retrospective studies have demonstrated the feasibility of using HR MRI to display the artery wall and lumen of the MCA. Using HR MRI, certain artery wall characteristics or plaque features, such as positive remodeling, intraplaque hemorrhage and large plaque burden, could potentially be used to identify high-risk patients requiring early prevention or needing more intensive treatments.⁴⁻⁸

Accordingly, the reproducibility and reliability of HR MRI for identifying artery wall characteristics and measuring the plaque burden of intracranial arterial atherosclerotic stenosis needs to be assessed. However, to our knowledge, only a few studies have investigated the reproducibility of HR MRI in evaluating intracranial atherosclerotic plaques.⁹⁻¹¹ In addition, detailed studies regarding intraobserver and interobserver reproducibility in characterizing MCA atherosclerosis has rarely been addressed.¹⁰ Furthermore, some of artery wall characteristics have not been investigated in these few published studies. In the present study, we aimed to determine the intraobserver and interobserver agreement not only by quantifying MCA wall and lumen areas but additionally to identify plaque surface morphology, plaque location and plaque components.

Patients and Methods

Patients

Between May 2014 and March 2017, we enrolled 69 patients with MCA stenosis from Zhongda Hospital affiliated Southeast University. All patients underwent the standard MRI/MRA or stroke MRI protocol to evaluate neurological symptoms or acute stroke. Inclusion criteria for patient enrollment included: (1) significant MCA stenosis (>30%) documented on MRA; (2) more than or equal to 2 risk factors (hypertension, diabetes mellitus, hyperlipidemia, cigarette smoking, and obesity) for atherosclerotic disease. Exclusion criteria for patient enrollment included: (1) coexisting ipsilateral internal carotid artery stenosis (>50%) on MRA; (2) presence of nonatherosclerotic vasculopathy, such as dissection, vasculitis, or moyamoya disease; (3)

evidence of cardio-embolism; (4) poor image quality secondary to motion artifacts.

The local Institutional Ethics Committee approved the study and written informed consents were obtained from all patients.

HR MRI Scanning

A 3.0T MR scanner (Siemens Magnetom Verio) with an 8-channel phased-array head coil was used. First, time-of-flight-MRA (TOF-MRA) was obtained in the axial plane and data were reconstructed using a dedicated online postprocessing tool to determine blood-vessel architecture. HR MRI, including black blood T1-weighted, T2-weighted, and proton density (PD)-weighted imaging was obtained for the stenotic site, as determined using the 3D TOF-MRA (Fig 1). Next, the 3D-MRA images and TOF source images were used as the localizer tomogram to ensure that the cross-sectional images were perpendicular to the M1 segment of the MCA. The above imaging sequences were applied with the following parameters.

TOF: repetition time (TR), 21 ms; echo time (TE), 3.6 ms; field of view, 200 × 160.4 mm; matrix size, 216 × 384; number of excitations (NEX), 1; slice thickness, 0.7 mm; and slice number, 150.

T1-weighted imaging: TR, 700 ms; TE, 26 ms; and NEX, 2.

T2-weighted imaging: TR, 2,800 ms; TE, 50 ms; and NEX, 4.

PD-weighted imaging: TR, 1,800 ms; TE, 29 ms; and NEX, 2.

All HR MRI scans were run with field of view, 140 × 140 mm; matrix size, 256 × 256; slice thickness, 2.0 mm; slice gap, 0.5 mm; and slice number, 9. The black blood technique with prerogional saturation pulses of 200% thickness to saturate the incoming arterial flow was used for all 3 scans.

Image Analysis

Morphology and signal intensity of the MCA plaques were analyzed against the signal intensity of the carotid artery and coronary artery plaque.¹²⁻¹⁴ Fibrous cap was defined as a high signal band adjacent to the lumen on T2-weighted images (Fig 1d). Recent and fresh intraplaque hemorrhage was characterized by an area of high signal intensity within the plaque, the intensity of which was more than 150% of the signal in adjacent muscles on T1-weighted images. Plaque surface irregularity was defined as a discontinuity of the plaque juxtalumenal surface and regularity defined as smooth inner wall (Fig 1c-e).⁸

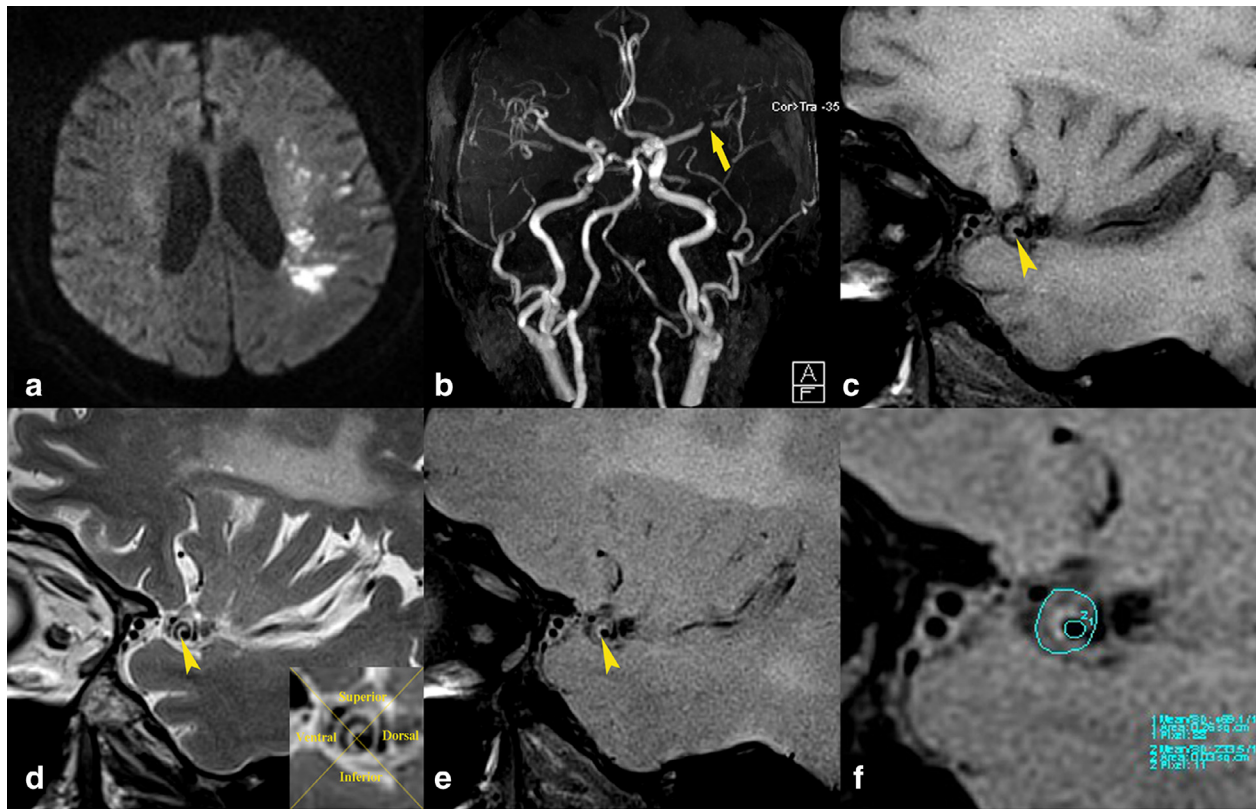


Figure 1. A 74-year-old woman had sudden onset of slurred speech with the right corner of mouth dropped. Diffusion weighted image showed multiple small infarcts in the left cortex and subcortical region (a). Severe stenosis of the left MCA stem was showed on MRA (b, straight arrow). The eccentric plaque located on the anterior and superior side was found on axial images of the MCA (c-f). The plaque distribution was evaluated by dividing the cross-section into 4 equal arcs (shown on the right lower corner of Figure (d)). The plaque surface was regular with smooth inner wall (c-e). The fibrous cap can be seen with arch-like hyperintense band adjacent to the lumen on T2-weighted image (d, arrowhead), corresponding to the area of iso-intense band on T1-weighted image (c) and hyperintense band on PD-weighted image (e). On the PD-weighted image magnified by 400%, the vessel and lumen boundary were manually traced and the area was measured (f).

Plaque distribution at the narrowest part of the lumen was evaluated by dividing the cross-section into 4 equal arcs, namely, the superior, inferior, dorsal, and ventral arcs, on the short axial T2-weighted images. The center of the grid was the geometric center of the lumen (Fig 1d). If a plaque was localized between 2 quadrants, the quadrant with the maximal plaque thickness was selected.^{15,16}

The plaque areas were measured on the short axial PD-weighted images using the software provided on the Siemens workstation (Fig 1f). After the images were magnified to 400%, the cross-sectional area of the MCA at the site of maximal lumen narrowing (MLN) and at a reference site (lesion-free or minimally diseased portions of the MCA proximal or distal to the stenosis) were measured. The MCA-cerebrospinal fluid interface was used to manually trace the vessel area (VA), and the blood-intima interface was used to trace the lumen area (LA). If the proximal reference site was abnormal, the neighboring distal site was used instead.

All images were first reviewed by 2 experienced readers who were blinded to the patients' clinical data. The wall characteristics, including plaque surface morphology,

plaque location, plaque components, and burden were identified and measured twice, 4 weeks apart, by 1 single reader.

Statistical Analysis

Intraobserver or interobserver reliability for the measurements and evaluation of the vessel wall was determined by kappa (k) value and intraclass correlation coefficient (ICC). Kappa value was calculated for dichotomous data. ICC was calculated with a one-way random effect for intraobserver continuous variables and a two-way random effect for interobserver continuous variables. The 95% confidence intervals (CIs) for all agreement parameters were calculated. Kappa values were graded based on the method by Landis and Koch (<0.0 = poor agreement; 0.0-0.2 = slight agreement; 0.21-0.40 = fair agreement; 0.41-0.60 = moderate agreement; 0.61-0.80 = substantial agreement; 0.81-1.0 = almost perfect).¹⁷ ICC more than 0.75 were considered as excellent agreement, 0.4-0.75 as moderate agreement, less than 0.4 as poor agreement.¹⁸ In addition, the Bland-Altman plot

method was used to assess the level of agreement for the area measurement.¹⁹

Results

In this study, 69 consecutive patients with moderate or severe MCA atherosclerotic stenosis underwent 3.0T HR MRI examinations. Five patients were excluded from the study due to their poor HR MRI image qualities attributed to motion artifacts. The 64 eligible patients included in this study had the median age of 65 years (range, 51-77 years). Eighteen (59%) were men. And the mean degree of stenosis of atherosclerotic MCA was 51.72% (SD = 15.41). Among them, 39(60%) had a transient ischemic attack or ischemic stroke and 26 (40%) were asymptomatic.

Intraobserver and Interobserver Reliability for Identification of Wall Characteristics

Intraobserver and interobserver agreement were all substantial for the identification of plaque surface irregularity (intraobserver: $k = 0.741, 0.555-0.897$; interobserver: $k = 0.685, 0.490-0.843$). Substantial intraobserver and interobserver reproducibility were also found for intraplaque hemorrhage identification (intraobserver: $k = 0.654, 0.446-0.838$; interobserver: $k = 0.605, 0.369-0.792$). For the identification of plaque fibrous cap, intraobserver agreement was substantial ($k = 0.654$) and interobserver agreement was moderate ($k = 0.553$) (Tables 1 and 2).

For identification of plaques position, the total intraobserver and interobserver agreement were almost perfect (intraobserver: $k = 0.872, 0.763-0.958$; interobserver: $k = 0.808, 0.683-0.914$). However, for identifying ventral and inferior plaques, intraobserver and interobserver

agreement were slightly lower compared to the agreement for identifying superior and dorsal plaques. Substantial interobserver agreement was found for identifying ventral and inferior plaques ($k = 0.792$ and 0.787 , respectively) and almost perfect for identifying superior and dorsal plaques ($k = 0.833$ and 0.829 , respectively) (as shown in Tables 1 and 2).

Intraobserver and Interobserver Reliability for Plaque Quantification

Intraobserver and interobserver reproducibility was excellent for VA at the site of MLN (VA_{MLN}) (intraobserver: ICC = 0.886, 0.814-0.931; interobserver: ICC=0.855, 0.761-0.912) and moderate for LA at the site of MLN (LA_{MLN}) (intraobserver: ICC = 0.695, 0.498-0.815; interobserver: ICC = 0.558, 0.274-0.731) (Table 3). Bland-Altman analysis showed robust agreement for intraobserver and interobserver measurements on VA_{MLN} . However, the interval of agreement for the LA_{MLN} measurement was wide compared to the mean, especially for the interobserver agreement (Figs 2 and 3).

For VA and LA at the reference site ($VA_{reference}$ and $LA_{reference}$), intraobserver and interobserver reproducibility was excellent (as shown in Table 3). In addition, Bland-Altman plots showed minor absolute differences in intraobserver and interobserver measurements (Figs 2 and 3).

Discussion

In recent years, HR MRI has emerged as a tool to in vivo evaluate intracranial arterial diseases. However, reproducibility of MRI for characterizing MCA plaque components and measuring plaque volumes has rarely been addressed.¹⁰ Hence, it is essential to conduct in-depth studies on the

Table 1. Intraobserver reproducibility of HR MRI in identifying MCA wall characteristics

	Observer 1 (First reading)	Intraobserver			
		Observer 1 (Second reading)		Agreement	k (95%CI)
		Present	Absent		
Irregularity of surface	Present	22	5	88%	0.741 (0.555, 0.897)
	Absent	3	34		
Fibrous cap	Present	29	5	83%	0.654 (0.496, 0.841)
	Absent	6	24		
Intraplaque hemorrhage	Present	17	4	84%	0.654 (0.446, 0.838)
	Absent	6	37		
Plaque distribution				91%	0.872 (0.763, 0.958)
	Superior	Present	14	1	97%
Ventral	Absent	1	48	92%	0.829 (0.664, 0.965)
	Present	20	3		
Inferior	Absent	2	39	94%	0.833 (0.618, 0.963)
	Present	14	2		
Dorsal	Absent	2	46	98%	0.943 (0.815, 1.000)
	Present	10	0		
	Absent	1	53		

Table 2. Interobserver reproducibility of HR MRI in identifying MCA wall characteristics

	Observer 1 (First reading)	Interobserver			
		Observer 2		Agreement	k (95%CI)
		Present	Absent		
Irregularity of surface	Present	24	5	84%	0.685 (0.490, 0.843)
	Absent	5	30		
Fibrous cap	Present	20	5	78%	0.553 (0.334, 0.749)
	Absent	9	30		
Intraplaque hemorrhage	Present	15	6	83%	0.605 (0.369, 0.792)
	Absent	5	38		
Plaque distribution				86%	0.808 (0.683, 0.914)
	Superior	Present	14		
Ventral	Present	19	4	91%	0.792 (0.630, 0.937)
	Absent	2	39		
Inferior	Present	13	2	92%	0.787 (0.581, 0.950)
	Absent	3	46		
Dorsal	Present	9	1	95%	0.829 (0.572, 1.000)
	Absent	2	52		

reliability of in vivo HR MRI for the identification and quantification of MCA atherosclerotic plaques.

Recently, Yang et al investigated the reader agreement for component characterization and plaque area measurements in MCA using HR MRI at 3.0T.¹⁰ In Yang's study, substantial intraobserver and interobserver agreement was demonstrated for intraplaque hemorrhage identification. We observed similar results in the present study. The lower agreement for intraplaque hemorrhage identification was observed with MCA compared to the carotid artery, which was the focus in the previous study.²⁰ Compared to carotid artery plaques, the lower incidence of MCA intraplaque hemorrhage, the relatively smaller hemorrhagic volume in the small MCA plaque, and very complicated and muddled hemorrhagic signal intensities (which usually overlap with other components within the limited MCA plaque space) are likely explanations for the lower agreement. Furthermore, vulnerable plaques are characterized not only by intraplaque hemorrhage but also by plaque rupture associated with irregular surfaces.²¹⁻²³ Accordingly, the reliability of plaque surface morphology was addressed in our study, which Yang's study lacked. We found substantial intraobserver and interobserver agreement for identifying plaque surface irregularity. All these suggest that HR MRI could be a reliable tool for the identification of intraplaque hemorrhage and MCA plaque rupture. In addition, HR MRI could be used for risk stratification of ischemic events and longitudinal clinical trials.

Based on previous carotid artery studies, fibrous caps are observed as high signal bands adjacent to the lumen on T2-weighted images.^{12,13} However, hyperintense regions of plaques on T2-weighted images represent not only fibrous cap but also intraplaque hemorrhage.¹³ Hence, the

Table 3. Intraobserver and interobserver reproducibility of HR MRI in quantifying MCA plaques

	ICC (95%CI)	
	Intraobserver	Interobserver
VA _{MLN}	0.886 (0.814, 0.931)	0.855 (0.761, 0.912)
LA _{MLN}	0.695 (0.498, 0.815)	0.558 (0.274, 0.731)
VA _{reference}	0.888 (0.817, 0.932)	0.847 (0.750, 0.907)
LA _{reference}	0.851 (0.755, 0.909)	0.764 (0.611, 0.856)

LA_{MLN}, lumen area at the site of maximal lumen narrowing; LA_{reference}, lumen area at the reference site; VA_{MLN}, vessel area at the site of maximal lumen narrowing; VA_{reference}, vessel area at the reference site.

intensity and morphology of hyperintense foci adjacent to the lumen on T2-weighted images should be taken into account when identifying fibrous caps. Furthermore, the intensity and the shape of the fibrous cap will be more variable and complicated in vulnerable or ruptured plaques. Hence, it is not easy to distinguish fibrous caps from other plaque components on T2 weighted images. In the present study, substantial intraobserver agreement and moderate interobserver agreement were found for identifying fibrous caps in MCA plaques, and were similar to the results observed in Yang's study.¹⁰ The results highlight the difficulties in distinguishing a fibrous cap from other plaque components using 3.0T HR MRI. Much remains to be improved for HR MRI to confidently identify fibrous cap.

In the present study, the reproducibility to identify plaque position was also assessed, which was not the focus in the previous study. The total intraobserver and interobserver agreement were almost perfect in our study. However, for identifying ventral and

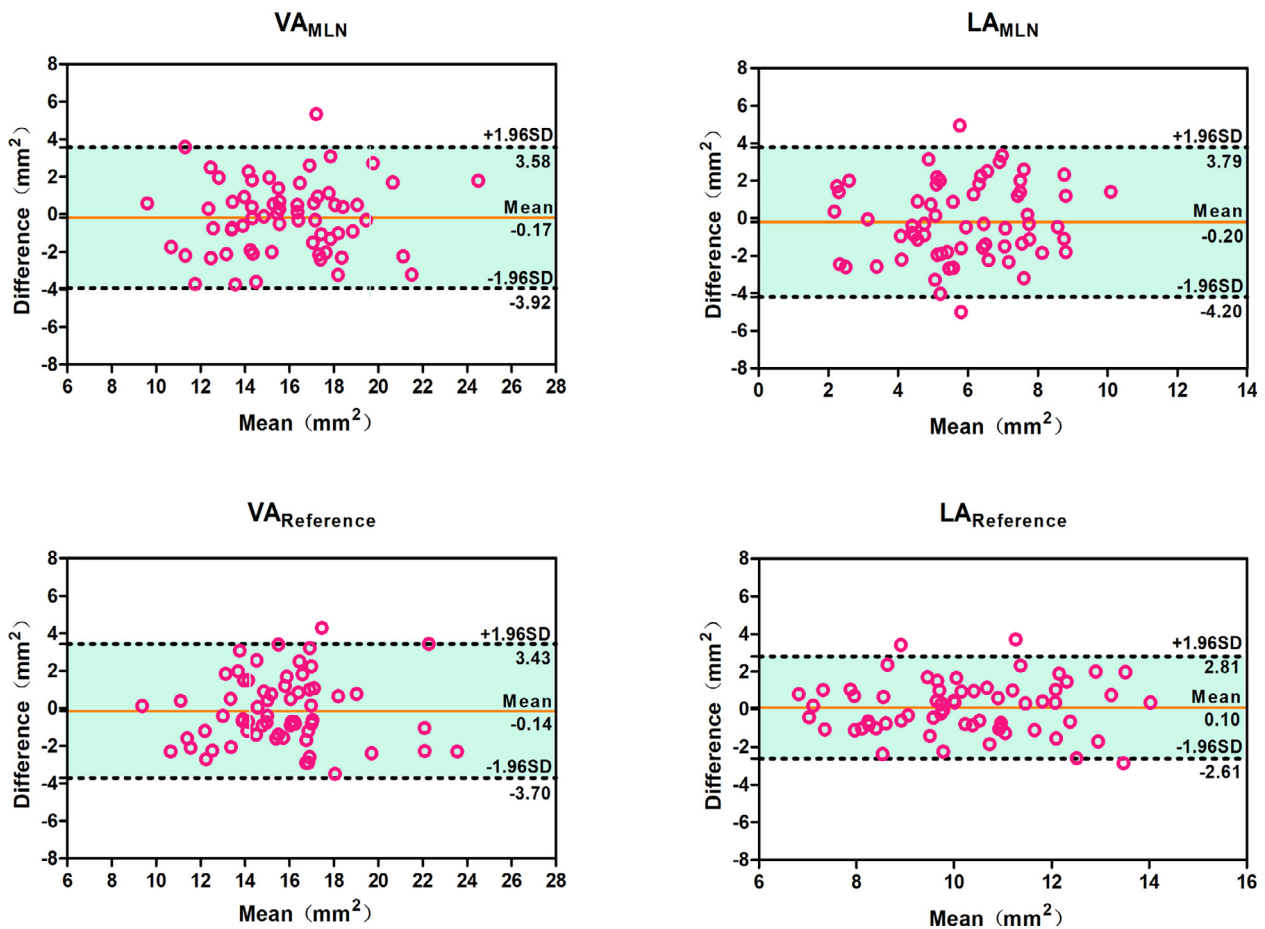


Figure 2. Bland-Altman plots of intraobserver reproducibility for vessel area (VA) and lumen area (LA) at the site of maximal lumen narrowing (MLN) and at the reference site.

inferior plaques, intraobserver and interobserver agreement were slightly lower compared to the agreement for identifying superior and dorsal plaques. The possible reasons may be as follows: MCA plaques were predominantly localized in the ventral and inferior walls which were demonstrated in the previous study,^{15,24} while larger plaques are usually localized on both the ventral and inferior walls. Hence there maybe more discrepancies between the observers in identifying ventral and inferior plaques compared to superior and dorsal plaques.

Regarding the reproducibility of MRI in quantifying vessel and lumen areas, we found that intraobserver and interobserver reproducibility were excellent for VA_{MLN}, VA_{reference}, and LA_{reference} measurements. However, the quantification for LA_{MLN} was not excellent. That may be due to plaque formation, small size of the luminal area, and complicated wall structure and the state of blood flow at the site of MLN. This will make it harder to decipher between the blood flow in the lumen and the inner surface of the plaque. Currently, preparation pulses could be used to obtain blood suppression, such as double

inversion recovery, motion-sensitizing preparation pulses, or delay alternating with nutation for tailored excitation preparation pulses.²⁵⁻²⁷ Although prerregional saturation pulse was used in our study, the intraobserver and interobserver reproducibility for HR MRI in quantifying LA_{MLN} was not excellent. This could be improved with higher field strength MRI and the new “black-blood” technique in the future.

Our study had several limitations. First, there was no pathological verification of the MCA wall components. Although no pathologic confirmation data were used in our study, MRI analysis of wall characteristics was carefully based on previous reports of carotid and coronary arterial stenosis. Furthermore, there are no critical disagreements from previous published studies. Second, several well-described limitations on the use of statistics influenced the interpretation of our results. Very low prevalence results in high levels of expected agreement; consequently, statistical values were low despite near perfect agreement as that was observed for dorsal plaques. Multicenter large cohort studies are needed to minimize the impact on the agreement.

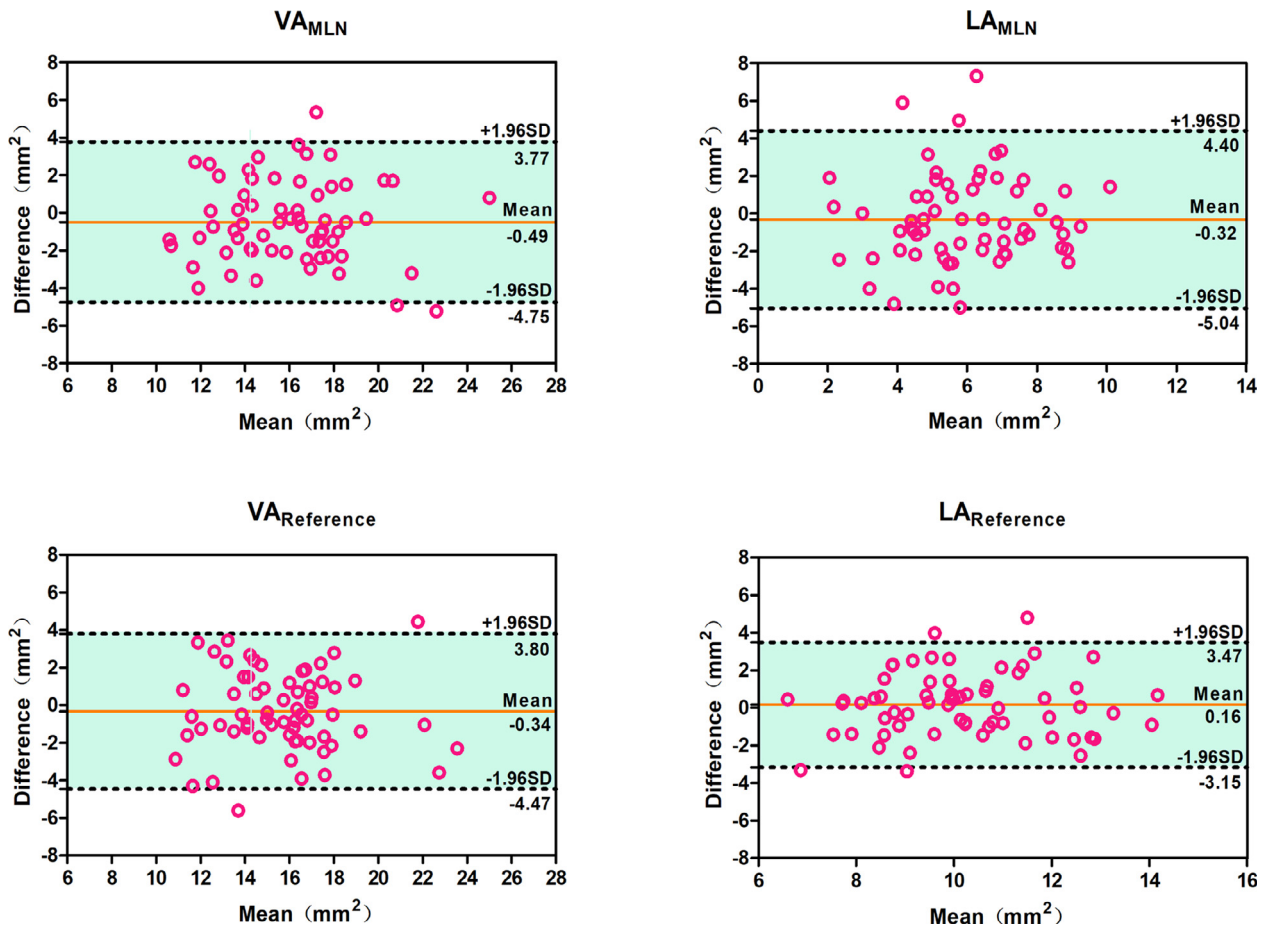


Figure 3. Bland-Altman plots of interobserver reproducibility for vessel area (VA) and lumen area (LA) at the site of maximal lumen narrowing (MLN) and at the reference site.

Conclusion

The reproducibility of 3.0T HR MRI for identification and quantification of artery wall characteristics were overall acceptable. However, with regards to HR MRI to identify fibrous cap and quantify LA_{MLN}, a large variability was present and hence the reliability of the technique needs to be improved.

Conflict of Interest

None.

References

- Suh DC, Lee SH, Kim KR, et al. Pattern of atherosclerotic carotid stenosis in Korean patients with stroke: different involvement of intracranial versus extracranial vessels. *Am J Neuroradiol* 2003;24:239-244.
- Kern R, Steinke W, Daffertshofer M, et al. Stroke recurrences in patients with symptomatic vs asymptomatic middle cerebral artery disease. *Neurology* 2005;65:859-864.
- Dieleman N, Ag VDK, Zwanenburg JJ, et al. Imaging intracranial vessel wall pathology with magnetic resonance imaging: current prospects and future directions. *Circulation* 2014;130:192-201.
- Ye Q, Anwar Z, Intrapromkul J, et al. Patterns and implications of intracranial arterial remodeling in stroke patients. *Stroke* 2016;47:434-440.
- Xu WH, Li ML, Gao S, et al. Middle cerebral artery intraplaque hemorrhage: prevalence and clinical relevance. *Ann Neurol* 2012;71:195-198.
- Xu WH, Li ML, Gao S, et al. In vivo high-resolution MR imaging of symptomatic and asymptomatic middle cerebral artery atherosclerotic stenosis. *Atherosclerosis* 2010;212:507-511.
- Zhao DL, Deng G, Xie B, et al. High-resolution MRI of the vessel wall in patients with symptomatic atherosclerotic stenosis of the middle cerebral artery. *J Clin Neurosci* 2015;22:700-704.
- Wu F, Song HQ, Ma QF, et al. Hyperintense plaque on intracranial vessel wall magnetic resonance imaging as a predictor of artery-to-artery embolic infarction. *Stroke* 2018;49:905-911.
- Ma N, Lou X, Zhao TQ, et al. Intraobserver and interobserver variability for measuring the wall area of the basilar artery at the level of the trigeminal ganglion on high-resolution MR images. *Am J Neuroradiol* 2011;32:29-32.

10. Yang WQ, Huang B, Liu XT, et al. Reproducibility of high-resolution MRI for the middle cerebral artery plaque at 3T. *Eur J Radiol* 2014;83:e49-e55.
11. Zhang X, Zhu C, Peng W, et al. Scan-rescan reproducibility of high resolution magnetic resonance imaging of atherosclerotic plaque in the middle cerebral artery. *PloS One* 2015;10:e0134913.
12. Winn WB, Schmiedl UP, Reichenbach DD, et al. Detection and characterization of atherosclerotic fibrous caps with T2-weighted MR. *Am J Neuroradiol* 1998;19:129-134.
13. Oppenheim C, Naggara O, Touzé E, et al. High-resolution MR imaging of the cervical arterial wall: what the radiologist needs to know. *Radiographics* 2009;29:1413-1431.
14. Altaf N, Macsweeney ST, Gladman J, et al. Carotid intraplaque hemorrhage predicts recurrent symptoms in patients with high-grade carotid stenosis. *Stroke* 2007;38:1633-1635.
15. Xu WH, Li ML, Gao S, et al. Plaque distribution of stenotic middle cerebral artery and its clinical relevance. *Stroke* 2011;42:2957-2959.
16. Huang B, Yang WQ, Liu XT. Basilar artery atherosclerotic plaques distribution in symptomatic patients: a 3.0T high-resolution MRI study. *Eur J Radiol* 2013;82:E199-E203.
17. Landis JR, Koch GG. The measurement of observer agreement for categorical data. *Biometrics* 1977;33:159-174.
18. Shrout PE, Fleiss JL. Intraclass correlations: uses in assessing rater reliability. *Psychol Bull* 1979;86:420-428.
19. Bland JM, Altman DG. Statistical methods for assessing agreement between two methods of clinical measurement. *Lancet* 1986;327:307-310.
20. Touze E, Toussaint JF, Coste J, et al. Reproducibility of high-resolution MRI for the identification and the quantification of carotid atherosclerotic plaque components consequences for prognosis studies and therapeutic trials. *Stroke* 2007;38:1812-1819.
21. Naghavi M, Libby P, Falk E, et al. From vulnerable plaque to vulnerable patient: a call for new definitions and risk assessment strategies: Part I. *Circulation* 2003;108:1664-1672.
22. Naghavi M, Libby P, Falk E, et al. From vulnerable plaque to vulnerable patient: a call for new definitions and risk assessment strategies: Part II. *Circulation* 2003;108:1772-1778.
23. Zhao DL, Deng G, Xie B, et al. Wall characteristics and mechanisms of ischaemic stroke in patients with atherosclerotic middle cerebral artery stenosis: a high-resolution MRI study. *Neurol Res* 2016;38:606-613.
24. Yoon Y, Lee DH, Kang DW, et al. Single subcortical infarction and atherosclerotic plaques in the middle cerebral artery: high-resolution magnetic resonance imaging findings. *Stroke* 2013;44:2462-2467.
25. Wang J, Yarnykh VL, Yuan C. Enhanced image quality in black-blood MRI by using the improved motion-sensitized driven-equilibrium (iMSDE) sequence. *J Magn Reson Imaging* 2010;31:1256-1263.
26. Wang J, Helle M, Zhou Z, et al. Joint blood and cerebrospinal fluid suppression for intracranial vessel wall MRI. *Magn Reson Med* 2016;75:831-838.
27. Lindenholtz A, van der Kolk AG, Zwanenburg JJM, et al. The use and pitfalls of intracranial vessel wall imaging: how we do it. *Radiology* 2018;286:12-28.